Pak. j. sci. ind. res. Ser. A: phys. sci. 2026 **69A**(2) 49-54 https://doi.org/10.52763/PJSIR.PHYS.SCI.69.2.2026.49.54

# Effect of Brazing Temperature and Bonding Time on the Microstructure and Mechanical Properties of 2024-T3 Alloy by Vacuum Furnace

**Mazin N. Ali*, Ahmed AlShuwaykh and Hadeel Safaa Hussein**
College of Engineering, Al-Iraqia University, Baghdad, Iraq

(received October 24, 2023; revised December 20, 2025; accepted December 22, 2025)

**Abstract.** In this study, the effect of different brazing temperatures with different bonding time on the microstructure and mechanical properties of aluminum alloy (AA2024-T3) in a vacuum furnace was investigated. The alloy was prepared and cut into a standard tensile specimen to braze a butt joint with a BAlSi filler metal. Vacuum brazing starts from preheating the specimens at 250 °C and 340 °C for 10 min and then brazing at 580 °C, 590 °C and 600 °C for 5, 10, 15 and 20 min followed by cooling inside the furnace. Results neglected the 5 min time with all temperature ranges because of insufficient bonding time, while the other specimens were successfully bonded. The microstructure and mechanical properties (tensile and hardness) were also studied. Finally, brazing temperature and bonding time significantly affected the microstructure and mechanical properties of the specimens because of the distribution of Si during brazing and the formation of some Al-Cu-Si phases and relevant eutectic and pro-eutectic phases. The cycle furnace design controlled the appearance of these phases. Moreover, the brazing temperature and bonding time contribute to the tensile and hardness of the brazed joint. Therefore, the specimens brazed at 600 °C for 20 min obtained the best mechanical properties that comes up with good properties in many applications, which also in future increased the uses of this process to join the refereed alloy.

**Keywords:** brazing temperature, bonding time, microstructure, mechanical properties, 2024 alloy, vacuum furnace

## Introduction

The 2024 aluminum alloy is used in different industrial applications such as automobile, aerospace and heat exchangers industries (Michael, 1993). Brazing is facing the complicated and hard assembling joints in different industries (Metals Handbook, 1990). Recently, brazing has been used in joining similar and dissimilar alloys, which added facilities and development in manufacturing (Shutov *et al*., 2020; Williams and Green, 2020). For aluminum alloys, brazing is the most favorable process (Sharma *et al*., 2015). In vacuum brazing, the most effective parameters that influence the final joint are filler metals, including the addition of elements, gap size, brazing temperature and brazing time; brazing sources and other metallurgical parameters such as wettability, filler density, viscosity and capillary motion (Davis, 1998). In addition, the factors related to Al/filler phases influence the mechanical properties of the final joint (John *et al*., 1996). Furthermore, there is an indirect factor during brazing such as the flow ability and fluidity (Matthew *et al*., 2020). Traditional Al-Si fillers such as BAlSi (3, 4, 5, 7 and 9) with maximum Si composition of about 13% have been commonly used for years (Shapiro, 2016). However, for many aluminum industries, such as 2024 alloy, the temperature range must be close to the solidus temperature between 570 °C and 610 °C (Li *et al*., 2012). Therefore, introducing novel low-melting fillers such as Al-Si fillers and using phase diagram calculations wisely are necessary to produce a good joint for many applications (Arash and Nastaran, 2021).

*Author for correspondence;
E-mail: mazin.n.ali@aliraqia.edu.iq

**Literature reviews.** In recent years, significant research has been conducted to study various aspects of aluminum alloy brazing. Notably, Weiyuan *et al*. (2021) investigated the microstructure and morphology of a Cu-Al joint brazed in a vacuum furnace. They identified three distinct regions, namely, the Cu side, Al side and central brazing region. The brazing area was primarily composed of $\alpha$-Al solid solution, $Cu_3Al_2$ and $CuAl_2$ metal compounds, with additional $\varepsilon$-$Cu_{15}Si_4$, Al-Si and $CuZn_2$ phases. These phases were dispersed in the brazing seam area in the form of acicular compounds (Weiyuan *et al*., 2021). Abood and Mohammed (2018) investigated the brazed AA5086-H116 with AISI316 stainless steel in atmospheric furnace using high-purity nitrogen and braze filler ER4047 and Er4043. Employing five holding times starts from 5 min increasingly to 5 min and ending in 25 min. Microstructural examination revealed two bounding layers: A Fe-rich layer on the stainless-steel side and an Al-rich layer on the aluminum side. The joint strength was primarily dependent on the thickness of these two layers. The EDS results showed significant diffusion between the fillers and the two metals, resulting in the formation of various intermetallic compounds. A clear correlation was found between the holding time and the diffusion of filler elements. The shear results of AA5086 with ER4047 filler was 18 MPa, whereas the result of joint with ER4043 was 16 MPa (Abood and Mohammed, 2018). Moreover, Huei *et al*. (2016) investigated the effect of four key parameters on the 6061-T6 joint, namely, heating temperature, heating time, brazing temperature and brazing time. After experimental work, the most dominant factor was soaking time. All the results analyzed using the Taguchi method indicated that the parameters optimally predicted the highest tensile strength. Excellent results were found in the prediction between the experimental and analysis results, with an error of only 0.33%, demonstrating the feasibility of the Taguchi method used in processing aluminum-brazed joints in vacuum furnaces. In addition, the microstructure, micro hardness and fractographs of the aluminum-brazed joints produced through an optimal process were analyzed (Huei *et al*., 2016). Motivated by the abovementioned considerations, gaining a comprehensive understanding of the relationship between the micro-structure and mechanical properties in vacuum-brazed joints using the traditional Al-Si fillers is crucial.

In this present study the AA2024-T3 were brazed in vacuum furnace brazing with different brazing temperatures (580, 590 and 600 °C) and with different bonding times (5, 10, 15, 20 min). Specimens were preheated to 250 °C and 340 °C for 10 min subsequently, three samples for each temperature range with three different bonding times conducted in vacuum brazing followed by furnace cooling. The microstructure and mechanical properties of butt joints with different brazing temperatures and bonding times using Al-Si filler metal were investigated.

## Material and Methods

Brazing the AA2024-T3 alloy in a vacuum furnace at different brazing temperatures (580 °C, 590 °C and 600 °C) for different bonding time periods (5, 10, 15 and 20 min) required the preparation of alloy from a plate (0.6 mm in thickness) that was cut by using a water jet machine into a standard tensile specimen and from the middle to form a butt gap, taking consideration the total length compared with the standard specimen in (Fig. 1). Filler foil of BAlSi (Al-12%Si) was selected as the most conventional filler metal. The chemical compositions of base and filler are presented in Table 1 this was done by chemical spectrometer device.

The vacuum pressure in a furnace was 10-2 torr with a heating rate of 20 °C/min to avoid surface carbon and hydrogen adsorption from the graphite walls inside the furnace. Heat cycle started from two steps: pre-heating at 250 °C and 340 °C for 10 min to conform the heat distribution inside the furnace (Fig. 2) and then increasing the temperature to 580 °C, 590 °C and 600 °C for 10, 15 and 20 min as shown in Table 2.

The 5 min bonding time was neglected for all specimens at all brazing temperature range because it fails in joining (Fig. 3).

Finally, the brazed specimens were cooled inside the vacuum furnace to room temperature and prepare them to mechanical and microstructural investigations. The tensile and microhardness tests were conducted on all specimens. The specimens were prepared for micro-structural examination by grinding, polishing and etching them in Keller's reagent (2.5 mL $HNO_3$, 1.5 mL HF and 95 mL water) at room temperature. The micro structure was studied using an optical microscope

**Fig. 1.** Langmuir plots for UCE and ECER.

**Table 1.** Chemical composition of base and filler metals

| Element | Si | Cu | Mg | Mn | Fe | Cr | Zn | Ti | Al |
|---|---|---|---|---|---|---|---|---|---|
| Wt.% | 0.05 | 4.19 | 1.37 | 0.56 | 0.14 | 0.019 | 0.06 | 0.019 | 93.64 |
| E4043 | 12 | | | | | | | | 88 |

**Table 2.** Systematic brazing of all samples with different temperatures and bonding time periods

| Sample name | B01 | B02 | B03 | B04 | B05 | B06 | B07 | B08 | B09 |
|---|---|---|---|---|---|---|---|---|---|
| Brazing temperature (°C) | 580 | 580 | 580 | 590 | 590 | 590 | 600 | 600 | 600 |
| Brazing time (min) | 10 | 15 | 20 | 10 | 15 | 20 | 10 | 15 | 20 |

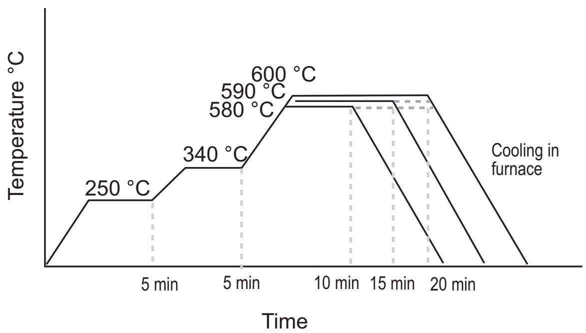


**Fig. 2.** Vacuum furnace heating and cooling cycle.

**Fig. 3.** Failure specimens after vacuum furnace brazing with 5 min bonding time.

**Table 3.** Stress and strain values of all specimens

| Specimen no. | Brazing temp. °C | Brazing time min. | Ultimate strength MPa | Strain % |
|---|---|---|---|---|
| Base | - | - | 460 | 13.7 |
| B01 | 580 | 10 | 370 | 11.9 |
| B02 | 580 | 15 | 388 | 11.71 |
| B03 | 580 | 20 | 397 | 11.9 |
| B04 | 590 | 10 | 360 | 11.7 |
| B05 | 590 | 15 | 378 | 11.9 |
| B06 | 590 | 20 | 388 | 11.9 |
| B07 | 600 | 10 | 389 | 12.0 |
| B08 | 600 | 15 | 410 | 12.11 |
| B09 | 600 | 20 | 446 | 12.7 |

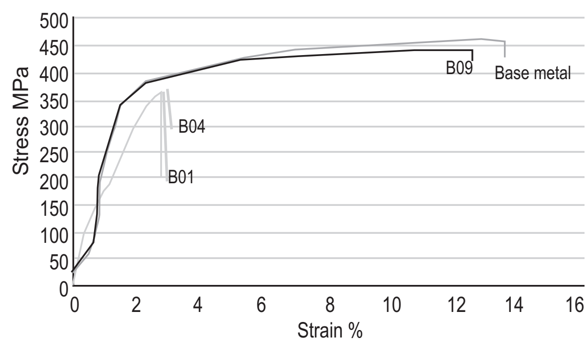


**Fig. 4.** Stress-strain diagram for base metals and vacuum-brazed specimens.

(OM/shimadzu) and SEM (Quanta FEG250) was used to investigate the microstructure supported with X-ray diffraction (XRD-D8 Discover).

## Results and Discussion

**Result of tensile test.** Tensile tests were performed on all specimens with a speed of 2 mm/s in accordance with the ASTM standard (Xiaoyue *et al*., 2022). Table 3 shows the value of ultimate stress and strain of all specimens. Specimen (no. B09) brazed at 600 °C for 20 min shows a perfect value near to the base metal tensile stress value.

The diagram shown in Fig. 4 indicates the convergence between the tensile values of base metal specimen and B09 specimen, whereas the remaining values of other specimens were taken randomly because of the low values that appeared in test.

**Result of hardness test.** The vickers micro-hardness test was conducted on all specimens and the weight was 300 g in 15 s (Alexander *et al*., 2016). The values of the micro-hardness of the braze zone, which is a region of the melted filler in the gap joint and the values of the interface zone, which is a region between the melted filler and the base alloy, are shown in Table 4. The comparison between the base metal and all specimens with different brazing temperatures and bonding time periods of both zones (braze and interface zones) is shown in Fig. 5.

**Result of optical microscope (OM).** The microstructure of brazed specimens and base metals after tensile test is observed in Fig. 6. Specimens were prepared, ground, polished and etched using Keller's reagent (2.5 mL of $HNO_3$, 1.5 mL HF and 95 mL water) (Pei-hao *et al*., 2019). The magnification was 100× and 200×. The microstructure of B09 is similar to that of a base metal and the different colors indicate the formation of at least two phases, while the other microstructure indicates the precipitation of Si around grain boundaries with some pores, which affect the tensile and hardness (Lyszewski *et al*., 2014).

**Result of SEM and XRD.** The SEM result of the B09 specimen before and after brazing, which was selected depending on the result of the mechanical properties that was nearest to the value of the base metal, is shown in Figs. 7 and 8. The XRD result of the B09 specimen and base metal is shown in Figs. 9 and 10.

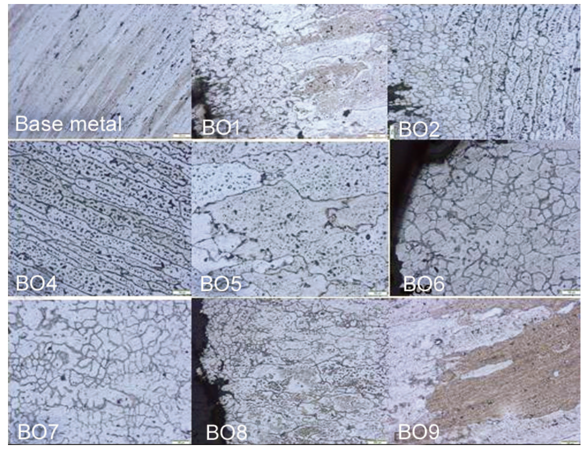


**Fig. 6.** Microstructure of base metals and vacuum-brazed specimens

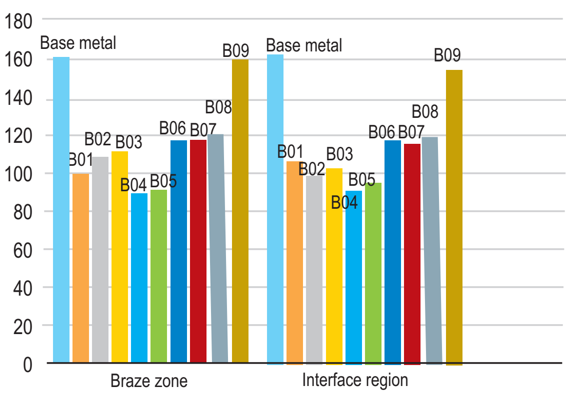


**Fig. 5.** Comparison between the micro-hardness of base metals and all vacuum-brazed specimens in the braze zone and interface zone.

This study systematically investigated vacuum brazing of 2024 alloy. Based on the results of this study, vacuum brazing of AA2024-T3 alloy was exposed to different brazing temperatures (580 °C, 590 °C and 600 °C) with different bonding time periods (10, 15 and 20 min). After the primary cycle furnace, the 5 min bonding time for all specimens was neglected because it fails to braze in all brazing temperature ranges. The microstructure and mechanical properties (tensile and hardness) were investigated in all specimens, which shows that the highest brazing temperature (600 °C) and longest bonding time (20 min) result in the highest values of

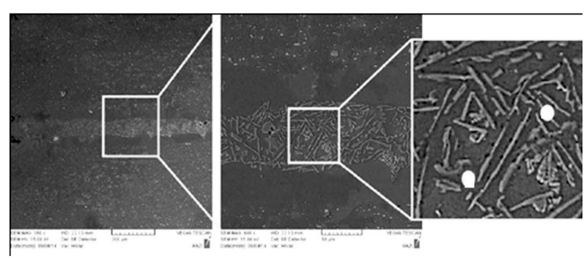

**Fig. 7.** Brazed zone before the tensile test.

**Table 4.** The values of Vickers micro hardness test

| Sample type | Base metal HMV | Vacuum brazing specimens (HMV) | | | | | | | | |
|---|---|---|---|---|---|---|---|---|---|---|
| | | B01 | B02 | B03 | B04 | B05 | B06 | B07 | B08 | B09 |
| Braze zone | 161 | 100 | 109 | 111 | 89.2 | 91.6 | 117 | 118.3 | 121 | 159 |
| Interface | 162 | 106 | 98.9 | 103.1 | 91 | 95.3 | 117.1 | 115.5 | 119 | 155.3 |

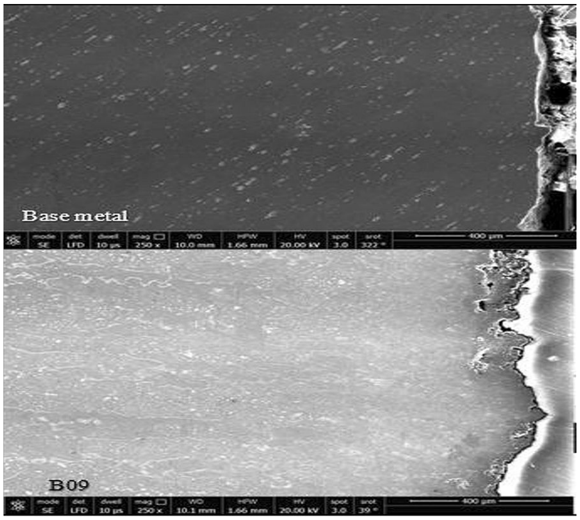


**Fig. 8.** Base metal and the B09 specimen vacuum brazed at 600 °C for 20 min.

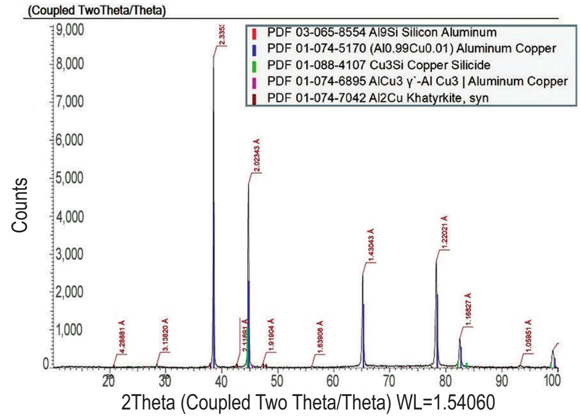


**Fig. 8.** XRD of the B09 specimen.

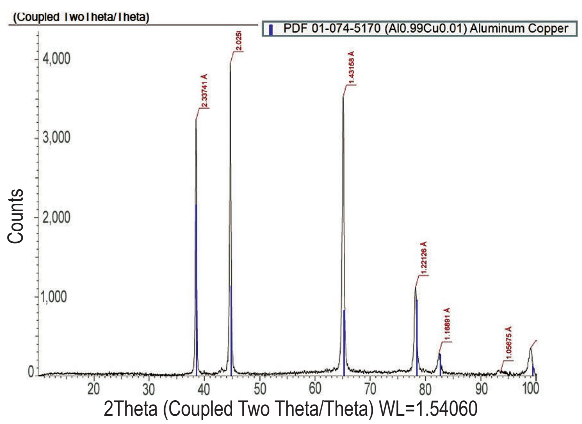


**Fig. 9.** XRD of the base metal.

tensile and hardness, which is near to the mechanical properties of base alloy (Tables 3 and 4 and Figs. 4 and 5). Other specimens brazed at 580 °C and 590 °C for 10, 15 and 20 min show similar tensile and hardness values because of the low solidus temperature of approximately 502 °C, making it difficult to braze for 5, 10 and 15 min especially with a conventional Al-12Si filler with a eutectic point of 577 °C and the addition of elements does not lower the eutectic point (Chankitmunkong *et al*., 2021; Guía-Tello *et al*., 2017). OM and SEM show an interfacial phase such as CuSi with sufficient amount of about 10% especially in B09, which could be clearly seen by XRD in Fig. 10. The SEM shows the formation of phases at the brazing zone (Fig. 7), which is close to the base alloy shown in Fig. 8. A mixture of phases appears in the brazing zone especially the CuSi, which breaks the layer of Al-Cu during brazing (Elsa *et al*., 2019; Mazin, 2018).

## Conclusion

1- This paper tried to fluctuation the researches by a study about vacuum brazing of 2024 alloy. Despite the difficulty of brazing, because of the type of alloy series, all specimens were subjected to a vacuum furnace with different brazing temperature and bonding time trying to reach the properties in standard alloy.
2- It has been founded that the perfect mechanical properties were specimen B09 (brazing temperature 600 °C and bonding time 20 min).
3- The SEM shows a huge simulation between B09 and based metal, means the sufficient temperature brazing and time affected the process.
4- A mixture of phases appears in brazing zone especially the (CuSi) that brake the layer of Al-Cu during the brazing process.
5- The (5 min) bonding time were neglected for all specimens due to failure brazing.

**Conflict of Interest.** The authors declare that they have no conflict of interest.

## References

Alexander, D., Hamerton, R., Cama, H., Greer, A. 2016. Investigating the alpha transformational solid-state phase change of dispersed intermetallic particles from an Al6(Fe, Mn) phase to an α-Al-(Fe,Mn)-Si phase. *Light Metals*, **22:** 1015-1020.

Abood, A.N., Mohammed, M.S. 2018. Furnace brazing of AA5086 aluminum alloy with AISI 316L stainless steel by ER4047 and ER4043 fillers. *Journal of King Abdulaziz University*, **29:** 35-47.

Arash, M., Nastaran, C. 2021. Concepts, procedures, and applications of artificial neural network models in streamflow forecasting. *Journal of Advances in Streamflow Forecasting*, **31:** 115-147.

Chankitmunkong, S., Limmaneevichitr, C., Kengkla, N., Eskin, D., Diewwanit, O. 2021. Effects of intermetallic removal on the anodic film and corrosion resistance of an A535 aluminum alloy. *Materials Today: Proceedings*, **42:** 1040-1045.

Davis, J.R. 1998. *Aluminum and Aluminum Alloys*: *Light Metals and Alloys*, 351-416 pp., Materials Park, Ohio, USA.

Elsa, M., Khorram, A., Ojo, O., Paidar, M. 2019. Effect of bonding pressure on microstructure and mechanical properties of aluminum/copper diffusion-bonded joint. *Sâdhanâ*, **44:** 126-131.

Guía-Tello, C., Trujillo-Vázquez, E. 2017. Furnace brazing parameters optimized by Taguchi method and corrosion behavior of tube-fin system of automotive condensers. *Journal of Materials Engineering and Performance*, **26:** 3901-3914.

Huei, L., Jiun-Ren, H., Chin-Ping, F. 2016. Optimization of vacuum brazing process parameters in AA6061 using Taguchi method. *Journal of Advanced Mechanical Design, Systems and Manufacturing*, **10:** 15-45.

John, M.H., Harold, M., Ho, C.Y. 1996. *Structural Alloys Handbook*, West Lafayette, USA.

Li, Y., Liu, W., Sekulic, D.P. 2012. Reactive wetting of AgCuTi filler metal on the TiAl-based alloy substrate. *Applied Surface Science*, **259:** 343-348.

Lyszewski, A.K., Elechowski, J.Z., Frontczak, A., Rutecki, P., Szymanski, W., Zamkotowicz, Z., Nowak, M. 2014. New rolled aluminum alloy products for the automotive industry. *Archives of Metallurgy and Materials*, **59:** 393-396.

Matthew, W., Jack, W., Russell, G. 2020. Brazing filler metals. *International Materials Reviews*, **6:** 257-285.

Mazin, A. 2018. Study the effect of ingate area on mechanical properties of as-cast (Al-0.4%Cu) using ANN. *Diyala Journal of Engineering Sciences*, **11:** 73-77.

ASM International Handbook Committee. 1990. *Properties and Selection: Nonferrous Alloys and Special-Purpose Materials*, 3470 pp., Materials Park, Ohio, USA.

Michael, B. 1993. *ASM Metals Reference Book*, 614 pp., Materials Park, Ohio, USA.

Pei-Hao, G., Guo-Liang, Q., Jun, Z., Chang-An, L. 2019. Parametric optimization and microstructural characterization of friction welded aeronautic aluminum alloy 2024. *Transactions of Nonferrous Metals Society of China*, **29:** 2483-2495.

Shapiro, A.E. 2016. Brazing of conventional titanium alloys. *ASM Handbook*, **16:** 36-43.

Sharma, A., Shin, Y.S., Jung, J.P. 2015. Influence of various additional elements in Al-based filler alloys for automotive and brazing industry. *Journal of Welding and Joining*, **33:** 30-35.

Shutov, I.V., Kamaeva, L.V., Krivilyov, M.D., Yu, C.N., Mesarovic, S., Sekulic, D.P. 2020. Effect of processing parameters on microstructure in brazing of Al-Si alloys. *Journal of Crystal Growth*, **53:** 25-28.

Weiyuan, Y., Tiandong, X., Wanwu, D., Xiaojun, W., Wenjun, Z. 2021. An investigation on vacuum brazing of dissimilar nonferrous metals of Cu and Al. *Advanced Materials Research*, **690:** 2565-2569.

Williams, R.B., Green, D. 2020. Influence of filler alloy on microstructures and properties of induction brazed Al/Cu joints. *Materials Science and Engineering A*, **76:** 142-153.

Xiaoyue, Z., Xuefeng, Z., Yong, Z., Xingbo, Z. 2022. The influence of the backing plate materials on microstructure and mechanical properties of friction spot extrusion brazing of AA2024-T3 aluminum alloy and brass sheets. *Journal of Manufacturing Processes*, **74:** 28-39.